IEICE Electronics Express, Vol.16, No.10, 1–6

LETTER

A novel, very low profile, dual band inverted 'E' monopole antenna for wireless applications in the laptop computer

Jayshri S. Kulkarni[1a)] **and Raju Seenivasan**[1]

Abstract A novel, very low profile and ultra-thin inverted 'E' shaped monopole antenna for WLAN/WiMAX applications in the laptop computer is presented. The thickness of the antenna is only 0.2 mm and is designed using only a pure copper strip of size $20 \times 6\,\mathrm{mm}^2$. The innovation of the design is miniaturized size and wider impedance bandwidth in dual band operation using two monopole radiating strips namely RS (inverted J) and PQ (inverted Z) along with open ended vertical tuning stub of size $4.5 \times 1\,\mathrm{mm}^2$. The measured impedance bandwidth spanned as 11.24% (2.35–2.63) GHz in a lower band (F_l) and 18.78% (4.92–5.94) GHz in the upper band (F_u) for VSWR < 2 and covers 2.4/5.2/5.8 GHz WLAN and 5.5 GHz WiMAX bands. The presented antenna has proved excellent radiation performance, including nearly omnidirectional patterns, a stable gain of around 4 dBi and an excellent efficiency of around 90% in F_l and F_u bands. This confirms the applicability for WLAN/WiMAX applications in the prominent ultra-thin laptop computers.

Keywords: inverted 'E' shaped monopole antenna, system ground, ultra-thin, WLAN, WiMAX
Classification: Microwave and millimeter-wave devices, circuits, and modules

1. Introduction

The Industrial Scientific Medical (ISM) bands, namely 2.4 GHz (2.40–2.48) GHz and 5 GHz (5.15–5.85) GHz are used in the WLAN/WiMAX environment. Therefore, multiband antennas including inverted-F [1, 2], the coupled-fed planar inverted-F antennas in [3, 4], branched monopole antenna [5], dual band monopole antenna [6], printed antenna [7], monopole antennas using reactive components [8, 9], antennas using additional ground plane [10, 11], meander antennas [12, 13], folded antennas [14, 15], uni-planar antennas in [16, 17, 18, 19], broadband antenna [20], antennas having thickness of 1 mm [21, 22, 23, 24] and cloverleaf-shaped monopole antenna [25] have been reported recently for WLAN/WiMAX technologies for the laptop computers. From the above mentioned antennas, it is understood that miniaturized and ultra-thin antennas showing high performance with less complex structure and covering WLAN/WiMAX bands for laptop applications are posing challenges for antenna designers due to shrinking of height and thickness of outside frame of the laptop display.

[1]Dept. of Electronics and Communication, Thiagarajar College of Engineering, Madurai-625015, India
a) jayah2113@gmail.com

DOI: 10.1587/elex.16.20190157
Received March 12, 2019
Accepted March 22, 2019
Publicized April 8, 2019
Copyedited May 25, 2019

This paper presents a novel, very low profile and ultra-thin, inverted 'E' shaped monopole antenna with an overall size $20 \times 6\,\mathrm{mm}^2$ and 0.2 mm thick only to operate in 2.4/5.2/5.5 GHz WLAN and 5.5 GHz WiMAX bands for wireless operations in the laptop computers [26, 27]. The presented prototype was first analyzed and then measurements were performed.

2. Antenna geometry and design

The schematic geometry of the presented antenna for WLAN and WiMAX operations in the laptop computer is shown in Fig. 1.

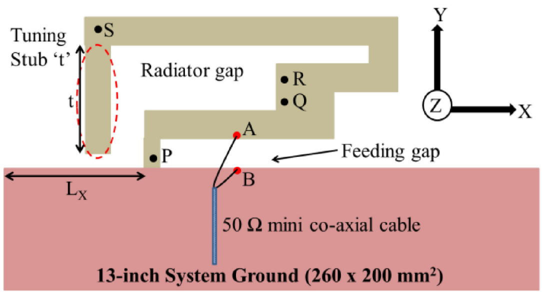

Fig. 1. Schematic geometry of the presented antenna

It consist of two radiating strips namely, strip RS (Inverted J) and strip PQ (Inverted Z) along with open ended vertical tuning stub of length 't'. The antenna is mounted on the system ground at point P and at a distance 'Lx'. The system ground is made up of 91% brass material that supports a 13-inch laptop display measuring $260 \times 200 \times 0.2\,\mathrm{mm}^3$. This structure adopts for small and low loss 50 Ω mini coaxial feed line, whose central conductor is connected at point 'A' on lower edge of strip PQ and grounding sheath soldered at point 'B' on the system ground. This feeding position introduces the feeding gap and makes the effective dielectric constant of all radiating strips equal to 1 [28], hence contribute in attaining the operating bands of the presented antenna.

The design steps of the presented antenna employed in CST MWS [29] are illustrated in Fig. 2 and the corresponding reflection coefficient (S_{11}) dB versus frequency results are shown in Fig. 3.

For forming the structure of Ant.1, as shown in Fig. 2(a), a simple short ended monopole radiating strip PQ (inverted-Z) whose length is approximately equal to a quarter wave long, to resonate at a frequency of 5.5 GHz is computed by using the following expression [30].

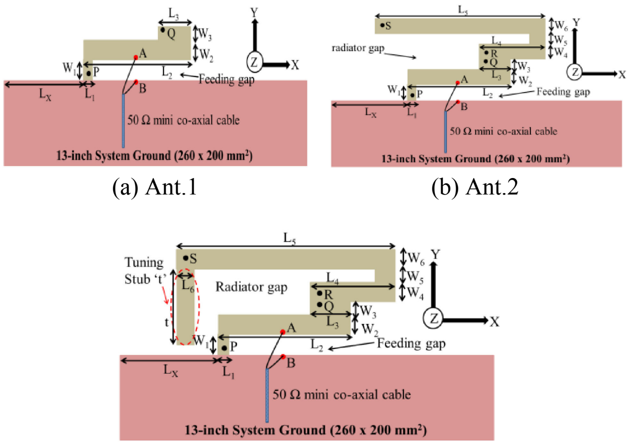

(a) Ant.1 (b) Ant.2

(c) Ant.3 (Presented Antenna)

Fig. 2. Complete design process of the presented antenna

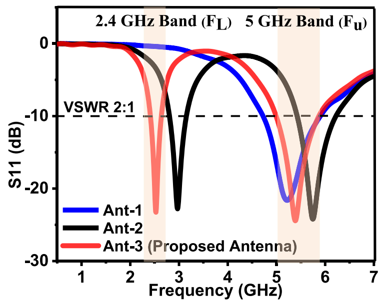

Fig. 3. Simulated reflection coefficient versus frequency for Ant.1, Ant.2 and Ant.3 (Ant. 3 being the presented antenna)

$$L = \frac{\lambda}{4} = \frac{C}{4f} \tag{1}$$

where, 'c' is the speed of light (m/s) and 'f' is resonating frequency. By using the above formula and optimization technique in CST, the length of strip PQ was optimized as 16 mm. The inductive reactance produced by strip PQ dominates the input impedance of Ant.1. This dominating inductive reactance is balanced by the opposite capacitive reactance, which is produced by feeding gap (W_1) at 5.5 GHz. Therefore, the maximum power transfer takes place due to proper impedance matching produced by the accurate dimension of feeding gap (W_1) and feeding positions. Hence, the Ant.1 successfully generates the resonance at 5.5 GHz with wider bandwidth as shown in Fig. 3. The wider bandwidth was achieved as the quality factor Q_0 of the antenna became very small. The Q_0 is defined as;

$$Q_0 = \frac{X}{R} = \frac{f}{BW} \tag{2}$$

where, X is reactance and R is the radiation resistance of the antenna. Due to proper impedance matching, the reactance is very small, approximately equal to 0 Ω and at the same time the value of R is also equal to 50 Ω. This makes the Q_0 of the Ant.1 very small which in turn widens the bandwidth. This proves that, the Ant.1 produces the resonance of 5.5 GHz with wider impedance bandwidth spanned in the range of (4.92–5.90) GHz as shown in Fig. 3.

Further, a monopole radiating strip RS (inverted J) which is approximately quarter wave long to resonate at 2.45 GHz, was computed using (1) and optimized using the CST optimization technique. The optimized length was 28 mm. The strip RS was coupled to Ant.1 connecting at point 'Q', without disturbing the feeding positions and creates a radiator gap as shown in Fig. 2(b). This complete structure is termed as the Ant.2. The radiator gap and the monopole radiating strip RS act as an electrical resonator due to shunt fed and this along with Ant. 1 exhibit the dual resonances at 2.9 GHz and 5.8 GHz as shown in Fig. 3. The impedance matching was disturbed at 2.45 GHz and 5.5 GHz due to the additional capacitive coupling offered by radiator gap and hence, Ant.2 was not able to cover the desired operating bands.

Finally, Ant.3 was designed to achieve proper impedance matching at desired resonances by protruding a vertical open ended tuning stub 't' at point 'S' without affecting the dual resonances, wider impedance bandwidth and compactness as shown in Fig. 2(c). The vertical tuning stub 't' controls the additional capacitive coupling by acting as a barrier for radiator gap and hence, contributes in shifting the resonance from 5.8 GHz to 5.5 GHz. At the same time, the length of stub 't' increases the path for electrical current which shifts the resonance from 2.9 GHz to 2.45 GHz. This Ant.3 covers two frequency bands, namely F_l (2.39–2.65) GHz and F_u (4.96–5.92) GHz with wide impedance bandwidths for VSWR < 2.

To further validate the wider bandwidth feature of Ant.3, Fig. 4(a) depicts the graph of input impedance Z_{in} versus frequency. In the operating bands F_l and F_u, proper impedance matching has been achieved due to correct feeding positions and accurate dimensions of W_1 and t. Hence, the input impedance remains stable around 50 Ω and reactance is approximately equal to 0 Ω. Therefore, according to equation (2), Q_0 of Ant.3 becomes very small which in turn widens the bandwidth in both the operating bands. From Fig. 4(b), it is also evident that due to excellent impedance matching, there are densely populated current paths in Ant.3, which means that several current paths have different electrical lengths. Merging of these current paths, results in decreasing Q_0 which further widens the bandwidth.

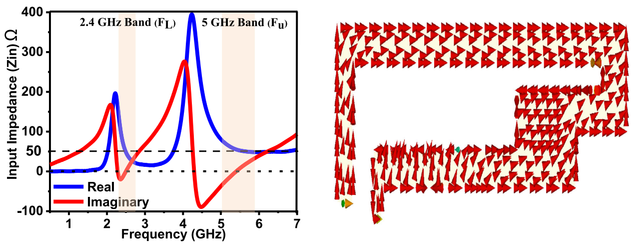

(a) (b)

Fig. 4. (a) Input Impedance vs Frequency (b) Current vector distribution of Ant. 3

In order to further validate the desired dual band characteristic of Ant.3, the simulated surface current distribution at 2.45 GHz and 5.5 GHz is shown and analyzed in Fig. 5. It is predominantly found that at 2.45 GHz, the maximum current flows through the strip RS and relatively small current flows through vertical tuning stub 't' which proves that strip RS and tuning stub ‘t’ contributes the Ant.3 to operate in F_l band, whereas at 5.5 GHz, the maximum current flows through the strip PQ and almost zero current flows through vertical tuning stub which proves that it only acts as a barrier which contributes the Ant.3 to operate in f_u band.

As Ant.3 operates in dual band with wider bandwidth and conforms to the requirement of WLAN and WiMAX operations in the laptop computers, it was selected for further testing and will be referred as presented antenna in the further section.

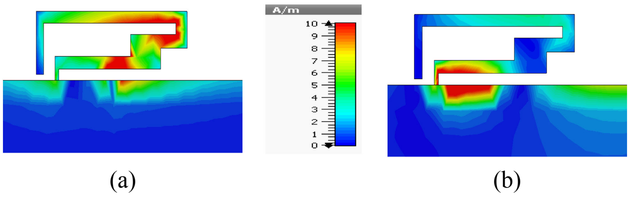

Fig. 5. Simulated surface current (A/m) distribution (a) at 2.45 GHz and (b) 5.55 GHz of the presented antenna

3. Parametric analysis

The important parameters selected for parametric analysis are an open ended vertical tuning stub ‘t’ and varying ‘L_x’ for mounting the presented antenna on the system ground. It also includes the analysis of ‘Effect of varying the sizes of system ground’ on S_{11} (dB) and impedance bandwidth across two bands of interest of the presented antenna to check its suitability for other portable devices.

3.1 The effect of varying length ‘t’ of tuning stub

The varying length ‘t’ mainly affects the resonances of operating bands. From Fig. 6, it is evident that as the value of ‘t’ increases, the resonance of 2.9 GHz and 5.8 GHz shift towards the lower frequency. At ‘t’ of 4.5 mm, the desired resonances of 2.45 GHz and 5.5 GHz are obtained with desired bandwidth.

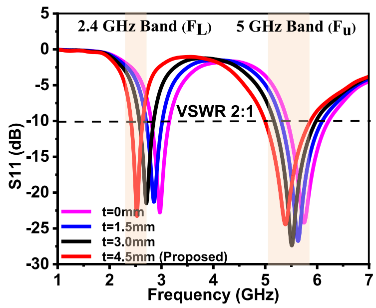

Fig. 6. Effect of varying ‘t’ on performance of the presented antenna

3.2 The effect of varying distance ‘Lx’

The effect of varying ‘L_x’ for mounting the presented antenna on the system ground, over F_l and F_u bands are analyzed in Fig. 7. It is confirmed that, mounting of the presented antenna at any place on the top edge of system ground, does not affect the performance of the presented antenna. In our design L_x is chosen to be 35 mm from left, by keeping in mind that the top left edge is normally reserved for installing the laptop assembly and center space is reserved for embedding the camera.

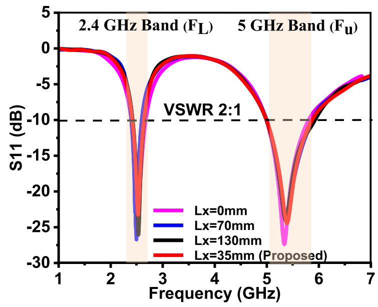

Fig. 7. Effect of varying ‘L_x’ on performance of the presented antenna

3.3 The effect of varying the sizes of the system ground

To contemplate the effect of varying sizes of the system ground (display screen) on the presented antenna, few standard sizes “5-inch” (Mobile), “10-inch” (Tablet/Notebook) and 14-inch” (Laptop) of display screen are compared with the existing system ground. Fig. 8 confirms that the presented antenna performs equally well for different sizes of the system ground with negligible effect on impedance bandwidth.

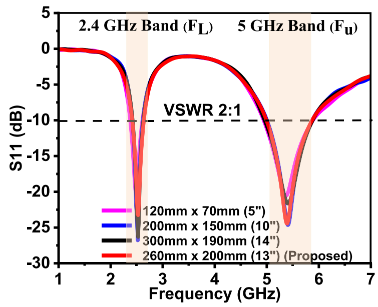

Fig. 8. Effect of varying size of system ground (display screen) on the performance of the presented antenna

Therefore, from the parametric study and using optimization technique in CST, the optimized parameters are specified in Table I.

Table I. Optimized parameters of proposed antenna.

Parameter	Value (mm)	Parameter	Value (mm)	Parameter	Value (mm)
L_1	0.5	L_6	1.0	W_4	1.2
L_2	14	L_x	35	W_5	1
L_3	4	W_1	1	W_6	1
L_4	7.5	W_2	1.1	T	4.5
L_5	17.5	W_3	0.6		

4. Experimental results and discussion

The presented prototype with optimal dimensions cataloged in Table I, was fabricated and tested as shown in Fig. 9. As discussed earlier coaxial cable was used for feeding as it is robust, offers convenience to select the feed point along with a good level of performance. A very small length of cable of 10 cm was used as smaller length of cable tends to smaller losses and higher performance. The diameter of coaxial cable was 1.8 mm with a maximum operating frequency up to 8 GHz. One probable factor to be considered while using coaxial cable is that the unbalanced current can flow through the outer conductor and form a standing wave on the feeding cable which further result in secondary radiation and affects the performance by increasing the losses and attenuation. In order to avoid this, the co-axial cable should be completely routed over the system ground. To do this, the most important parameter to be considered is the bending radius. Even though every co-axial cable has a bending radius, the bending should be as minimum as possible, as bending of coaxial cable can further increase the losses and attenuation, further affecting the performance, even if it is within the defined bending radius. Hence, the co-axial cable was routed with minimum bend to overcome the effect of standing waves and to get maximum performance. A network analyzer up to 16 GHz was used to measure VSWR and S_{11} (dB). The radiation performance, including radiation patterns, gain and radiation efficiency were measured in the calibrated anechoic chamber of size $8 \times 4 \times 4\,m^3$.

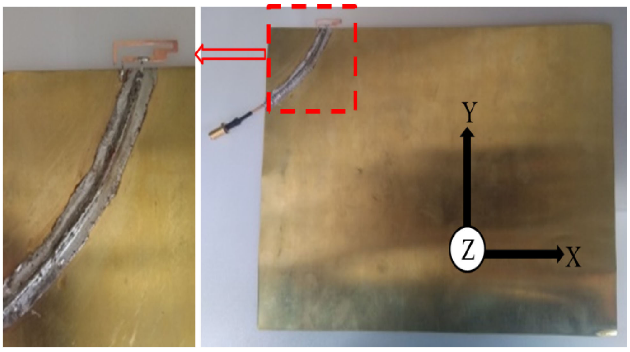

Fig. 9. Fabricated photo of the presented antenna

4.1 Characteristics of S_{11} (dB)

Fig. 10 presents the simulated and measured S_{11} (dB) values of the presented antenna and their comparison in Table II. A minimal deviation is observed which may be due to soldering and fabrication tolerance. However, both the simulated and measured F_l and F_u bands cover 2.4/5.2/5.8 GHz WLAN and 5.5 GHz WiMAX bands with wider bandwidth.

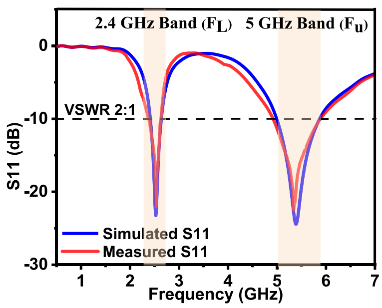

Fig. 10. Comparison of simulated and measured reflection coefficient

Table II. Comparison of S_{11} (dB) and operating bands of the presented antenna for VSWR < 2

	Amplitude (dB)		Operating Bands (GHz)	
	F_l	F_u	F_l	F_u
Simulated	−23	−25	2.39–2.65	4.96–5.92
Measured	−22	−23	2.35–2.63	4.92–5.94

4.2 Radiation patterns

A good agreement between simulated and measured radiation patterns of the presented antenna in the x-y plane at 2.45 GHz and 5.5 GHz is found in Fig. 11. At these frequencies, the measured patterns are smooth and clean due to proper routing of coaxial cable. E_θ patterns are bidirectional and radiate more energy in a horizontal direction which ensures maximum energy for WLAN/WiMAX applications in the laptop computer, whereas E_ϕ radiation patterns are nearly omnidirectional and hence, can be used for broad coverage of the area.

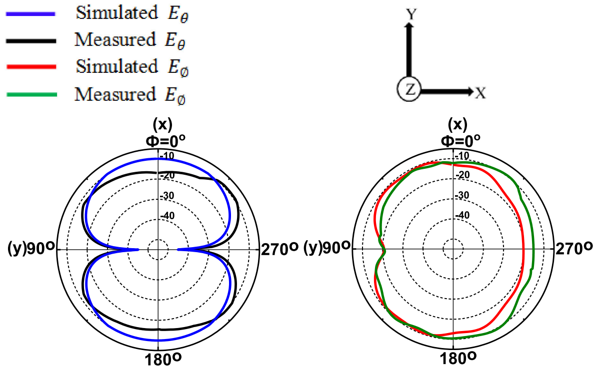

(a) at 2.45 GHz (x-y plane)

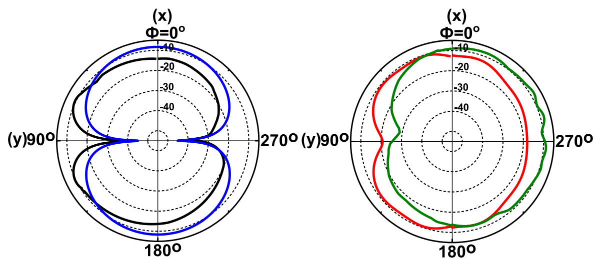

(b) at 5.5 GHz (x-y plane)

Fig. 11. Simulated and measured radiation patterns in x-y plane

4.3 Simulated and measured gain and efficiency

The gain measurement requires same facility as radiation pattern measurement and is based on Friss transmission equation as expressed in (3).

$$G_{2dB} = 20log_{10}\left(\frac{4\pi r}{\lambda}\right) + 10log_{10}\left(\frac{p_2}{p_1}\right) - (G_{1dB}) \quad (3)$$

where, G_{2dB} and G_{1dB} are gain of presented and the reference antenna respectively, r is distance between the reference and presented antenna, p_2 and p_1 are received and transmitted power of presented and reference antenna, respectively.

The simulated and measured values of gain and efficiency for the presented antenna are graphically expressed in Fig. 12 and their comparison in Table III. A small deviation between simulated and measured values is seen because, simulation is done under ideal conditions. This deviation can be acceptable for wireless operations in the laptop computers. However, Table III concludes that the presented antenna exhibits stable gain and excellent efficiency in both operating bands F_l and F_u, proving that it has a good signal reception quality which is required for wireless operations in the laptop computer.

Table III. Comparison of simulated and measured gain and efficiency

Operating bands (GHz)	Gain (dBi)		Efficiency (%)	
	Simulated	Measured	Simulated	Measured
F_l	4.30–4.35	4.09–4.26	93.00–94.00	91.22–93.20
F_u	4.06–4.45	3.93–4.25	92.43–94.00	89.44–91.00

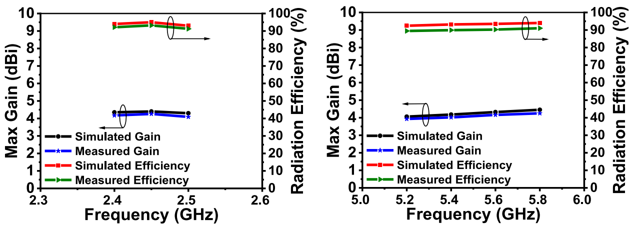

(a) (b)

Fig. 12. Simulated and measured gain and efficiency of the presented antenna (a) in F_l band (b) in F_u band

5. Concluding remarks

A novel, very low profile and ultra-thin inverted 'E' shaped monopole antenna $20 \times 6 \times 0.2\,mm^3$ exhibits the measured wide impedance bandwidth of 11.24% (2.35–2.63) GHz in lower band (F_l) and 18.78% (4.92–5.94) GHz in the upper band (F_u) for VSWR < 2. Hence, the presented antenna covers the standard bandwidth requirement of 2.4/5.2/5.8 GHz WLAN and 5.5 GHz WiMAX bands for wireless applications in the laptop computer. It also satisfies the required radiation performance for the desired F_l and F_u bands confirming good quality of signal reception for wireless operations in the laptop computers. Therefore, because of a very low profile, ultra-thin, low cost, better performance and faster time to market, the presented antenna is a good candidate for modern ultra-thin laptops.

References

[1] L. Pazin and Y. Leviatan: "Inverted-F laptop antenna with enhanced bandwidth for Wi-Fi/WiMAX applications," IEEE Trans. Antennas Propag. **59** (2011) 1065 (DOI: 10.1109/TAP.2010.2103036).
[2] H.-W. Liu, *et al.*: "Compact inverted-F antenna with meander shorting strip for laptop computer WLAN applications," IEEE Antennas Wireless Propag. Lett. **10** (2011) 540 (DOI: 10.1109/LAWP.2011.2157887).
[3] C.-T. Lee and K.-L. Wong: "Uniplanar printed coupled-fed PIFA with a band-notching slit for WLAN/WiMAX operation in the laptop computer," IEEE Trans. Antennas Propag. **57** (2009) 1252 (DOI: 10.1109/TAP.2009.2015843).
[4] S.-J. Liao, *et al.*: "Small-size uniplanar coupled-fed PIFA for 2.4/5.2/5.8 GHz WLAN operation in the laptop computer," Microw. Opt. Technol. Lett. **51** (2009) 1023 (DOI: 10.1002/mop.24206).
[5] L.-Y. Chen and K.-L. Wong: "2.4/5.2/5.8 GHz WLAN antenna for the ultrabook computer with metal housing," Proc. of APMC 2012 (2012) 322 (DOI: 10.1109/APMC.2012.6421585).
[6] L.-C. Chou and K.-L. Wong: "Uni-planar dual-band monopole antenna for 2.4/5 GHz WLAN operation in the laptop computer," IEEE Trans. Antennas Propag. **55** (2007) 3739 (DOI: 10.1109/TAP.2007.910501).
[7] M. Abioghli: "Dual-band two layered printed antenna for 2.4/5 GHz WLAN operation in the laptop computer," IEICE Electron. Express **8** (2011) 1519 (DOI: 10.1587/elex.8.1519).
[8] T.-W. Kang and K.-L. Wong: "Very small size printed monopole with embedded chip inductor for 2.4/5.2/5.8 GHz WLAN laptop computer antenna," Microw. Opt. Technol. Lett. **52** (2010) 171 (DOI: 10.1002/mop.24843).
[9] S.-W. Su: "Very-low-profile, 2.4/5-GHz WLAN monopole antenna for large screen-to-body-ratio notebook computers," Microw. Opt. Technol. Lett. **60** (2018) 1313 (DOI: 10.1002/mop.31156).
[10] L. Pazin, *et al.*: "Multiband flat-plate inverted-F antenna for Wi-Fi/WiMAX operation," IEEE Antennas Wireless Propag. Lett. **7** (2008) 197 (DOI: 10.1109/LAWP.2008.920848).
[11] C.-Y.-D. Sim, *et al.*: "Uniplanar antenna design with adhesive ground plane for laptop WLAN operation," IEEE Antennas Wireless Propag. Lett. **13** (2014) 337 (DOI: 10.1109/LAWP.2014.2305837).
[12] M. Naser-Moghadasi, *et al.*: "Highly compact meander line antenna using DGS technique for WLAN communication systems," IEICE Electron. Express **8** (2011) 722 (DOI: 10.1587/elex.8.722).
[13] H.-Y. Chien, *et al.*: "Dual-band meander monopole antenna for WLAN operation in laptop computer," IEEE Antennas Wireless Propag. Lett. **12** (2013) 694 (DOI: 10.1109/LAWP.2013.2263373).
[14] L.-C. Chou, *et al.*: "A small size internal dual-band metal-strip antenna for 2.4/5 GHz WLAN operation in the laptop computer," IEEE APSURSI (2008) (DOI: 10.1109/APS.2008.4619456).
[15] C.-T. Lee and S.-W. Su: "Very-low-profile, stand-alone, tri-band WLAN antenna design for laptop-tablet computer with complete metal-backed cover," IEEE APCAP (2016) 189 (DOI: 10.1109/APCAP.2016.7843162).
[16] C.-Y.-D. Sim, *et al.*: "A novel uniplanar antenna with dual wideband characteristics for tablet/laptop applications," Int. J. RF Microw. Comput.-Aided Eng. **27** (2017) e21145 (DOI: 10.1002/mmce.21145).
[17] H.-W. Liu and C.-F. Yang: "Miniature multiband monopole antenna for WWAN operation in laptop computer," Electron. Lett. **46** (2010) 21 (DOI: 10.1049/el.2010.3254).
[18] R. Khan, *et al.*: "Multiband monopole antenna with minimised ground plane influence for portable devices," IET Microw. Antennas Propag. **11** (2017) 1829 (DOI: 10.1049/iet-map.2016.1084).
[19] S.-W. Su, *et al.*: "Compact paper-clip-shaped wire antenna for 2.4 GHz and 5.2 GHz WLAN operation," Microw. Opt. Technol. Lett. **50** (2008) 2572 (DOI: 10.1002/mop.23760).
[20] Y. Liu, *et al.*: "A broadband dual-antenna system operating at the WLAN/WiMAX bands for laptop computers," IEEE Antennas Wireless Propag. Lett. **14** (2015) 1060 (DOI: 10.1109/LAWP.2015.2394473).
[21] K.-L. Wong, *et al.*: "Dual-band flat-plate antenna with a shorted parasitic element for laptop application," IEEE Trans. Antennas Propag. **53** (2005) 539 (DOI: 10.1109/TAP.2004.838754).
[22] T. Kim, *et al.*: "Internal dual-band WLAN antenna for laptop applications," IEEE APSURSI (2010) (DOI: 10.1109/APS.2010.5561725).
[23] Y. Xu, *et al.*: "Compact CPW-fed printed monopole antenna with triple-band characteristics for WLAN/WiMAX applications," Electron. Lett. **48** (2012) 1519 (DOI: 10.1049/el.2012.3255).
[24] H. Huang, *et al.*: "Multiband metamaterial-loaded monopole antenna for WLAN/WiMAX applications," IEEE Antennas Wire-

less Propag. Lett. **14** (2014) 662 (DOI: 10.1109/LAWP.2014.2376969).
[25] I.-P. Hong and I.-G. Lee: "Design of a film antenna using a cloverleaf-shaped monopole structure for WiBro and WLAN," IEICE Electron. Express **9** (2012) 654 (DOI: 10.1587/elex.9.654).
[26] N. C. Zhi: *Antennas for Portable Devices* (John Wiley & Sons Ltd., 2007).
[27] R. C. Johnson: *Antenna Engineering Handbook* (McGraw-Hill Inc., 1993) 3rd ed.
[28] G. Kumar and K. P. Ray: *Broadband Microstrip Antenna* (Artech House, Inc., 2003).
[29] CST-Computer Simulation Technology Studio Suite, 2017, https://www.cst.com/2017.
[30] C. A. Balanis: *Antenna Theory Analysis and Design* (John Wiley & Sons, Inc., Hoboken, New Jersey, 2005) 3rd ed.